

PAPER

[View Article Online](#)
[View Journal](#)

Cite this: DOI: 10.1039/d5fb00147a

Rosemary oil infused bionanocomposite films:
a sustainable and active packaging material for
paneer preservationBhavya E P ^{ab} and Maya Raman ^{*a}

The present study investigates the development of bionanocomposite films formulated using carrageenan (1.9% w/v), soy protein (0.3% w/v) and nanocellulose (2% w/v), with rosemary essential oil (REO, 1–2% v/v) incorporated as a bioactive agent. The incorporation of 2% REO significantly reduced the tensile strength (23.7 MPa) but increased elongation at break (19.8%), enhancing flexibility. The hydration properties decreased (moisture content 15.5%, swelling capacity 14.5%, water vapour transmission rate $644.4 \text{ g m}^{-2} \text{ 24 h}^{-1}$), confirming superior moisture barrier performance. Fourier-transform infrared spectroscopy indicated strong polymer–polymer interactions, while SEM revealed oil droplet dispersion within the matrix. The films with 2% REO showed the highest antimicrobial activity, notably against *Bacillus cereus* (25 mm inhibition zone), attributable to phenolic constituents (α -pinene, 1,8-cineole, camphor). The films achieved 90% soil biodegradability after 28 days, underscoring their environmental sustainability. The application studies demonstrated that paneer packaged in 2% REO films maintained superior quality during 28 days of refrigeration (4 °C), with lower moisture (42.8%), titratable acidity (0.7%), tyrosine content (23 mg/100 g), improved colour (L^* -75.2, a^* -3.5, b^* -19.2) with textural parameters, hardness (69 N) and chewiness (9.8 N) respectively. Overall, carrageenan/soy protein/nanocellulose films with REO represent a multifunctional, biodegradable, and sustainable system for active food packaging.

Received 12th April 2025
Accepted 18th October 2025

DOI: 10.1039/d5fb00147a

rsc.li/susfoodtech

Sustainability spotlight

Sustainability has become a central focus in the development of next generation packaging materials, prompting increased research into biodegradable and ecofriendly alternatives. This study presents the formulation of a sustainable high performance bionanocomposite film composed of carrageenan, soy protein, nanocellulose and rosemary oil, each selected for their natural origin and environmental compatibility. The resulting film not only supports sustainability through their biodegradability but also exhibit enhanced physicochemical, antioxidant, and antimicrobial properties. The findings suggest that these carrageenan/soy protein/nanocellulose/rosemary oil-based bionanocomposite films hold strong potential as active food packaging materials. The developed packaging material represents a promising step toward greener food packaging, aligning with Sustainable Development Goals (SDGs) 3 (Good Health and Well-being) and 12 (Responsible Consumption and Production). Its multifunctionality contributes not only to environmental protection but also to food preservation and safety, aligning with global efforts to minimize waste and promote a more sustainable food system.

1 Introduction

Conventional food packaging materials are generally derived from petroleum-based polymers. These provide essential functions such as ensuring food safety, preserving quality, being lightweight, offering effective barrier properties, and providing good heat-sealability, which make them suitable for packaging applications. However, these plastics are non-degradable, non-recyclable, and have raised significant environmental concerns. The continued reliance on fossil-derived resources for their production further exacerbates environmental sustainability challenges associated with conventional polymers. In

response, extensive research is being carried out to develop alternative, sustainable packaging solutions, with a particular focus on biopolymers.¹

Biopolymers, derived from renewable resources such as plants, animals and microorganisms are extensively studied as sustainable and eco-friendly alternatives to conventional petroleum-based plastics. Their inherent non-toxicity, biocompatibility and biodegradability make them particularly suitable for food packaging applications. In comparison with petroleum-based polymers, biopolymers are sourced from renewable feedstocks, thereby reducing reliance on fossil fuels and mitigating the environmental challenges.² Biopolymers such as polysaccharides (starch, chitosan, cellulose), proteins (gelatin, soy protein, casein) and lipids, as well as their blends, have been extensively explored for designing food packaging materials with improved functional and barrier properties. However, the

^aDepartment of Food Science & Technology, Kerala University of Fisheries & Ocean Studies, Ernakulam, India. E-mail: ramanmaya@gmail.com

^bDepartment of Food Processing Technology St. Teresa's College, Ernakulam, India



widespread adoption of biopolymers in packaging is limited due to the challenges in thermal, barrier and mechanical properties. Marine-based polysaccharides such as alginates, carrageenan and agar are gaining attention due to their gel-forming ability, versatility and biodegradability.³ Among these, carrageenan, from red seaweed (*Kappaphycus alvarezii*), comprising sulphated galactans, has been extensively studied for its high strength, gelling characteristics and superior film-forming ability, thus making it a promising option for sustainable packaging solutions.⁴ Soy protein, another notable biopolymer, exhibits high gas and oil barrier properties at lower relative humidity and excellent film-forming capacity. However, the commercial applications of soy protein-based films remain restricted due to their low mechanical strength and high water sensitivity. These drawbacks can be mitigated by enhancing the physicochemical and mechanical properties of the films through blending with suitable biopolymers, plasticizers, and nanofillers.⁵ Moreover, recent progress in nanotechnology has demonstrated significant potential for further improving the physicochemical and functional properties of the biopolymer films.

Nanocomposites represent a promising approach to enhance the performance of biopolymer-based films for food packaging applications by improving the thermal, barrier and mechanical properties. The incorporation of nanoparticles (nanocellulose and nanofillers) strengthens the films by promoting strong interfacial interaction with the biopolymer matrix mainly through hydrogen bonding.⁶ Nanocellulose derived from cotton linters exhibits a higher aspect ratio, increased surface area, superior physical and chemical properties, along with excellent colloidal stability, structural strength and film-forming ability, thus making it suitable for reinforcing the biopolymer films.

Furthermore, the incorporation of antimicrobial agents, including bacteriocins, enzymes, and essential oils, enhances the functional performance of biopolymer films by inhibiting pathogenic microorganisms, thereby contributing to active food preservation and shelf-life extension.⁷ Plant-derived essential oils, recognized as GRAS (Generally Recognized as Safe) have garnered significant attention for their antimicrobial and antioxidant properties. Rosemary essential oil (*Rosmarinus officinalis* L.) is relatively less explored and studied compared to clove, thyme or oregano oil. The phenolic-rich rosemary oil is characterized by its unique diterpenes (carnosic acid, carnosol and rosmarinic acid), which exhibit both antioxidant and antimicrobial properties, making it effective in prolonging the shelf life of perishable products (paneer).⁸

Earlier studies have extensively investigated bionanocomposite films based on starch, chitosan and gelatin incorporating essential oils such as thyme and clove, primarily focusing on their antimicrobial and barrier functions. The present study introduces a novel hybrid system that combines carrageenan, a sulfated polysaccharide with strong gelling ability; soy protein, a protein-rich biopolymer with favorable permeability characteristics; and nanocellulose, a nanofiller known to reinforce mechanical strength.

The effects of individual components (carrageenan, soy protein, nanocellulose and rosemary essential oil) are well

documented in the literature; however, their integration into a single bionanocomposite film has not been previously reported. The novelty of the study lies in strategic integration of these into a single multifunctional hybrid system that offers synergistic performance that goes beyond the performance of individual components. The C/SP/NC matrix provides a robust structural framework and film forming ability, while the incorporation of REO confers additional bioactivity and barrier enhancement. Unlike other biopolymer-essential oil composites, this formulation demonstrates a balance of mechanical integrity comparable to certain conventional plastics, improved surface hydrophobicity for better moisture resistance, and multifunctional bioactivity, including antioxidant and antimicrobial properties.

The rosemary oil (REO) remains underexplored, despite its unique phytochemical profile, antioxidant activity, milder sensory attributes and regulatory acceptance. The systematic impact of REO on film functionality, microbial stability and sensory property of dairy products are still lacking. Previous reports demonstrate the individual benefits of biopolymers and the essential oil, but their synergistic integration to achieve a balanced improvement in mechanical integrity, barrier protection, and bioactivity has not been adequately addressed.

Therefore, this study was designed to fill this knowledge gap by developing and characterizing optimized C/SP/NC films incorporated with REO at varying concentrations. We hypothesize that the inclusion of REO will not only enhance the antioxidant and antimicrobial functionalities of the film but also modulate their physical, morphological, and barrier properties, thereby providing a novel, multifunctional active packaging system capable of extending the shelf life of paneer. Paneer, a dairy product produced through acid-heat coagulation, is highly perishable, retains quality for only one day at ambient temperature and about six days under refrigeration.⁹ This research also focuses on evaluating the physical, structural, morphological, mechanical and functional properties of the bionanocomposite films while determining their effectiveness in maintaining the quality of paneer throughout storage. The present study also provides a significant advancement in the development of a sustainable food packaging system.

2 Materials and methods

2.1 Materials

Carrageenan ($M_w \approx 551.8 \text{ g mol}^{-1}$) was procured from Marine Hydrocolloids Ltd, Kochi. The nanocellulose (nanocrystalline with 6% w/w cellulose, viscosity of 0.060 at 23 °C) was procured from ICAR-Central Institute for Research on Cotton Technology (CIRCOT, Mumbai), India. The defatted soya chunks with less than 1% oil were purchased from a local market (Kochi, India). Rosemary oil was procured from Green Leaf Extractions, Kochi, India. The analytical-grade solvents and chemicals were purchased from Sigma-Aldrich (Bangalore, India).

2.2 Preparation of bionanocomposite film

The bionanocomposite films (carrageenan/soy protein/nanocellulose) were produced using the method of solvent



Table 1 Experimental conditions used to formulate the bionanocomposite films through the casting method^a

Films	C (g)/w/v%	SP (g)/w/v%	NC (g)/w/v%	Glycerol (g)/w/v%	REO (g)/w/v%
R0.0	1.9/1.9	0.3/0.3	1.5/1.5	0.8/0.8	0
R1.0	1.9/1.9	0.3/0.3	1.5/1.5	0.8/0.8	0.045/1
R1.5	1.9/1.9	0.3/0.3	1.5/1.5	0.8/0.8	0.0675/1.5
R2.0	1.9/1.9	0.3/0.3	1.5/1.5	0.8/0.8	0.09/2

^a Carrageenan-C; soy protein-SP; nanocellulose-NC; rosemary essential oil-REO. The weight content (w%) of REO in the C/SP/NC solutions was established and the concentration expressed in w/v% in 100 mL solution.

casting¹⁰ with slight modifications. The experimental conditions for film preparation are summarized in Table 1. Carrageenan (1.98 g), soy protein (0.3 g), nanocellulose (1.5 g) and glycerol (0.8 g) were dissolved in distilled water (100 mL) under mechanical stirring (Model Remi, 1 MLH, 150 W, Mumbai) at 400 rpm and heated (80 ± 5 °C) in a water bath for 30 min until complete solubilization. The rosemary essential oil (REO, 1%, 1.5%, and 2%, v/v) was then added the solution and homogenized using a stirrer (15 min, 30 °C)¹¹ (Table 1). The selection of REO concentrations was based on the literature reports and preliminary trials with higher and lower concentrations. The homogenate was poured into the Petri dishes (10×10 cm) and tray dried (IG-125HAO-220V, Delhi, 40 ± 2 °C, 48 h). The dried films were packed in zip-locked polyethylene bags and stored at ambient temperature (30 °C and 75% RH) until further analysis.

2.3 Characterization of films

2.3.1 Moisture content, swelling capacity and water solubility. The moisture content (MC) of the bionanocomposite films was estimated at with slight modifications.¹² Briefly, the films (2×2 cm) were oven-dried (105 °C, 24 h) using a hot air oven (Labline Instruments, Kochi), until a constant weight was attained. The tests were carried out in triplicate, and the MC (%) was calculated by eqn (1):

$$\text{Moisture content (\%)} = \frac{W_1 - W_2}{W_1} \times 100 \quad (1)$$

where, W_1 = initial weight of the film, W_2 = final dry weight of the film.

The swelling capacity (SC) of the films was calculated,¹³ with slight modification. Briefly, the dried films (4×4 cm) were immersed in distilled water (20 mL) and subjected to equilibration (15 min, 37 °C, 84% RH). The SC (%) was calculated by eqn (2):

$$\text{Swelling capacity (\%)} = \frac{W_2 - W_1}{W_1} \times 100 \quad (2)$$

where, W_1 = initial weight of the film, W_2 = final weight of the film.

The water solubility of the bionanocomposite films was determined gravimetrically¹⁴ with slight modification. Briefly, the film of size 20 mm \times 20 mm was oven-dried at 103 °C for a day to achieve constant weight, and the initial dry weight was noted as W_1 . The film was then immersed in distilled water for 24 h and stored at ambient temperature (25 °C). The films were removed from water and dried in a hot air oven at 104 °C for

24 h, and the final weight of the film was noted as W_2 . The tests for each film were carried out in triplicate. The weight loss or solubility percentage of the films was calculated from the eqn (3) given below.

$$\text{Water solubility (\%)} = \frac{W_2 - W_1}{W_1} \times 100 \quad (3)$$

2.3.2 Thickness and mechanical strength. The thickness of the bionanocomposite films ($n = 5$) was determined using a digital micrometer (Mitutoyo, USA, precision: 0.001 mm). The thickness measurements of the film samples were carried out in triplicate.¹²

The mechanical properties (tensile strength, TS, and elongation at break, EB) of the films were measured by a texture analyzer (M/s Lloyd Instrument, Ltd, Fareham, UK) according to ASTM D 882-02 (2002) method.¹⁵ The films were cut into rectangular size (80 mm \times 50 mm) and clamped with an initial clamping distance at 50 mm. The stretch rate was maintained at 25 mm min⁻¹. According to eqn (4) and (5), TS and EB were calculated for the triplicate samples.

$$\text{Tensile strength (MPa)} = \frac{F_{\max}}{\phi} \quad (4)$$

where, F_{\max} = maximum load (N), ϕ = cross-sectional area (m²).

Elongation at break (EAB) was calculated using the following equation:

$$\text{Elongation at break} = \frac{\Delta L}{l_0} \times 100 \quad (5)$$

where, ΔL = increase in length of the film, l_0 = initial length of the film.

2.3.3 Color and opacity of the films. The, L^* (lightness), a^* (redness), and b^* (yellowness) values of the bionanocomposite films were measured in triplicate using a colorimeter (Colour flex EZ, Hunterlab, USA). The difference in color (ΔE) was calculated according to eqn (6):

$$\Delta E = \sqrt{(\Delta L^*)^2 + (\Delta a^*)^2 + (\Delta b^*)^2} \quad (6)$$

where, L^* , a^* , and b^* indicate the color parameters of the film, $\Delta L^* = L^* - L_o$, $\Delta a^* = a^* - a_o$ and $\Delta b^* = b^* - b_o$ in which L_o , a_o , and b_o represent the color parameter values of the standard.

The absorbance values of the film samples were carried out in triplicate at 600 nm were measured using a UV-visible spectrophotometer (M/s Jasco V-730, India)¹⁶ and the opacity (A mm⁻¹) was calculated according to eqn (7):



$$\text{Opacity (A mm}^{-1}\text{)} = A_{600}/x \quad (7)$$

where, A_{600} = absorbance of the sample at 600 nm, x = film thickness (mm).

2.3.4 Water vapour transmission rate (WVTR) and oxygen transmission rate (OTR). The water vapour transmission rate (WVTR) was estimated by an automatic water vapour testing machine (SYSTEESTER, China). The preconditioned films for 24 h were placed in the chamber at ambient temperature (37 °C) and 90% RH. The instrument measured the amount of water vapor passing through the sample over a 24 h period. The weight was continuously monitored and WVTR was calculated for the triplicate samples and expressed in $\text{g m}^{-2} \text{ day}^{-1}$.

The oxygen transmission rate (OTR) was analyzed as per ASTM D-3985-81 by using qn oxygen permeability analyzer (OX-TRAN, 2/21, MOCON, USA). The 24 h preconditioned film was mounted in the gas diffusion cell to create a sealed barrier between the two chambers. The test was conducted under controlled conditions (23 °C and 60% relative humidity) with 100% oxygen on one side of the film and hydrogen (2%) and nitrogen (98%) on other side. The OTR was calculated for the triplicate samples based on the amount of oxygen that permeates through the film in 24 h and is expressed in $\text{cm}^{-2} 24 \text{ h}^{-1}$.

2.3.5 X-ray diffraction studies (XRD). The X-ray diffraction analysis of the bionanocomposite films was performed using a tabletop diffractometer (Miniflex 600, Rigaku, Wilmington, MA, USA). Utilizing a copper target $\text{Cu K}\alpha$ ($\lambda = 0.154 \text{ nm}$), the following parameters were set: voltage of 40 kV, current of 20 mA, scanning range (2θ) of 3–400.¹⁷

2.3.6 Fourier transform infrared spectroscopy (FTIR). The FTIR spectral analysis of the bionanocomposite films was performed using an FTIR spectrophotometer (Thermo Nicolet iS 50 FTIR spectrophotometer, USA) at a resolution 0.2 cm^{-1} in the range 400–4000 cm^{-1} .¹⁵ The analysis was carried out in the attenuated total reflectance mode (ATR) by directly analyzing the films on a diamond crystal.

2.3.7 Scanning electron microscopy (SEM) and atomic force microscopy (AFM). The surface morphology of the bionanocomposite films was determined using a scanning electron microscope (SEM-JEOL, model JSM 6460LV, Tokyo, Japan), and the film surface topography was analysed using atomic force microscopy (Bruker Dimension Edge SPM, USA).³ The films were gold sputtered (JEOL-JFC-1600, Japan), mounted on the steel stubs with double-sided carbon-tape, and SEM images were acquired at an accelerating voltage of 20.0 kV. Briefly, the film ($2 \times 2 \text{ cm}$) morphology was measured using AFM contact mode with high-frequency sensors (1.85 V). The images were captured in Peak Force Tapping mode using 0.1 M KCl, a standard quartz liquid cell, and a silicon nitride cantilever with a nominal spring constant of 0.7 N m^{-1} , a tip radius of 2 nm, and a resonance frequency of 150 kHz (SCANASYST-FLUID+, Bruker, USA). The measurements were performed at room temperature and RH (27 °C and 65% RH). Image analysis was conducted, and root mean square surface roughness (R_q) was calculated using NanoScope Analysis 1.5 Software.

2.3.8 Water contact angle. The water contact angle of the bionanocomposite films ($15 \times 15 \text{ mm}$) was evaluated using

a goniometer.¹⁸ The films were placed on a glass slide and a drop of water (5 μL) was applied on the film surface using an automatic piston syringe and photographed (U1 series Super speed digital camera in supramolecule mode). The contact angle was determined using the DROP image Advanced v 2.8 software. The contact angles were determined on both sides of the drops and three to five independent measurements were averaged.

2.3.9 Thermal properties. The thermal properties (thermogravimetric analysis, TGA and differential scanning calorimetry, DSC) of bionanocomposite films were determined using STA7300RV (Hitachi, Japan) and Netzsch DSC 204 F1 (Wittelsbacherstraße, Germany), respectively. Briefly, the weight loss (%) of the bionanocomposite films (10 mg) was determined by heating from 40 to 760 °C at the rate of 20 °C min^{-1} under an inert environment. The films (10 mg) were placed in sealed DSC aluminium pans, with an empty sealed pan as reference. The melting temperature was measured using DSC under a continuous flow of inert nitrogen (150 mL min^{-1}) at a temperature range of (40 °C to 760 °C).¹⁹

2.3.10 Antimicrobial and antioxidant properties. The antimicrobial activity of the films against pathogenic organisms were determined using the method of disc diffusion with slight modifications.²⁰ Different strains of Gram-positive (*Bacillus cereus* MTCC 430 and *Staphylococcus aureus* ATCC 25923) and the Gram-negative (*Escherichia coli* ATCC 8739 and *Salmonella typhi* ATCC 14028) bacteria were tested in this study. The microbial cells were cultured in nutrient broth at 37 °C for 18 h; and the cells were collected and spread on Mueller Hinton agar plates ($1.5 \times 10^8 \text{ CFU mL}^{-1}$). The film discs (2 cm diameter) were placed on plates inoculated with test microorganisms, and then incubated (Labline Bacteriological Incubator, Model: LSC-30A; 37 °C, 24 h). The antibiotic disc gentamicin (2 cm diameter) was used as the positive control. After incubation, the microbial growth inhibition zone diameters were measured.

The 2,2-diphenyl-1-picrylhydrazyl (DPPH) radical scavenging capacity was performed using the spectrophotometric method, with slight modification.²¹ Briefly, film immersed in ethanol solution (2 mL) was incubated with DPPH solution (2 mL, 0.1 w/v) for 30 min in the dark at ambient temperature (37 °C) and the absorbance (A_{517}) was measured using a spectrophotometer (M/s Jasco V-730, India). The DPPH antioxidant activity was calculated and expressed as percentage inhibition. The IC_{50} (concentration at 50% DPPH reduction) was also calculated.

2.3.11 Soil burial degradation study. The pre-weighed dried films ($3 \times 3 \text{ cm}$) were buried in the soil (obtained from KUFOS, Kochi, $9^{\circ}54'37'' \text{ N}$ and $76^{\circ}19'2'' \text{ E}$) at a depth of 10 cm.²² These were carefully removed at regular intervals (4, 8, 16, 20, 24 and 28 days), cleaned to remove the adhering soil, and dried in a tray dryer (IG-125HAO-220 V, Delhi; 40 °C, 15 min) until constant weight was achieved. The percentage of weight loss was calculated for the triplicate samples using the following eqn (8).

$$\text{Weight loss (\%)} = \frac{W_0 - W_A}{W_0} \times 100 \quad (8)$$

where, W_0 -initial weight of the film, W_A -weight after each testing period.



2.3.12 Preservation performance of paneer. The study included a comprehensive assessment of the effects of the film formulation on the preservation of the shelf life and quality of paneer. Paneer (50 g) was wrapped in C/SP/N-based bionanocomposite films incorporated with REO (2%) and bionanocomposite film with REO (0%) served as the control. The wrapped paneer cubes were stored at refrigeration condition (4 °C) for 30 days. The moisture content, titratable acidity, tyrosine content, color and textural properties were evaluated at regular intervals (3 days).

2.3.12.1 Determination of moisture content and titratable acidity. The moisture content of the paneer was determined according to the AOAC method.²³ Briefly, paneer (5 g) was oven-dried (Lab line Instruments, Kochi) at 105 °C for 4 h, and the moisture content was determined in triplicate from the weight difference.

The titratable acidity of paneer was estimated by the titration method.²⁴ Briefly, the sample (10 g) was thoroughly homogenized with 100 mL of distilled water and an aliquot was titrated against NaOH (0.1 N), using phenolphthalein as an indicator. The titratable acidity was determined in triplicate and the value was expressed as the percentage of lactic acid.

2.3.12.2 Determination of tyrosine content. The paneer (20 g) was blended with TCA solution (20%, 100 mL) and the filtrate was collected. An aliquot (2.5 mL) was further mixed with distilled water, NaOH (0.5 N, 10 mL) and 3 mL of Folin-Ciocalteu reagent diluted 1 : 2 with distilled water. The mixture was incubated in the dark for 30 min, and the optical density (OD) was determined at 730 nm, using tyrosine as the standard. The experiment was performed in triplicate, and the tyrosine content was expressed as mg tyrosine/100 g of paneer.²⁵

2.3.12.3 Determination of color and textural properties. The colour parameters, L^* , a^* and b^* were estimated for paneer using a colorimeter (Lovibond LC-100 Spectro colorimeter, UK). The hardness and chewiness of paneer were determined using a texture analyzer (EZ-Shimadzu).²⁶ The cubes (50 g) were compressed twice to 75% of their original height at a crosshead speed of 0.05 cm s^{-1} , with the second compression occurring at 5 s after the first, with the sample at ambient temperature ($25 \pm 1^\circ \text{C}$).

2.3.13 Statistical analysis. The experiment was carried out in triplicate and the mean \pm standard deviation was used to describe the results. The statistical analysis was performed by using the software Wasp 2.0 (Web Agri Stat Package) for Windows formulated by the ICAR-Central Coastal Agricultural Research Institute in New Delhi, India. To assess the data, a one-way ANOVA was conducted by using Tukey's significant difference test, based on a significant difference of $p < 0.05$.

3 Results and discussion

3.1 Bionanocomposite film characteristics

3.1.1 Moisture content, swelling capacity and water solubility. Bionanocomposite films containing carrageenan, soy protein and nanocellulose, incorporated with rosemary essential oil, were used to develop an eco-friendly packaging system. The incorporation of rosemary essential oil (REO) showed a progressive reduction in moisture content (20.8 to 15.5%) and

Table 2 Physico-chemical properties of carrageenan-soy protein-nanocellulose-based bionanocomposite film incorporated with rosemary essential^a

Film	MC (%)	SC (%)	Solubility (%)	Thickness (μm)	TS (MPa)	Color				Opacity (A mm^{-1})	OTR ($\text{cm}^{-2} \text{ 24 h}^{-1}$)	WVTR ($\text{g m}^{-2} \text{ 24 h}^{-1}$)
						EAB (%)	L^*	a^*	b^*			
R0.0	$23.4 \pm 0.4^*$	$21.3 \pm 0.1^*$	$41.2 \pm 0.2^*$	$80.6 \pm 0.2^*$	$31.6 \pm 0.1^*$	13.2 ± 0.1	$83.2 \pm 0.2^*$	$3.0 \pm 0.1^*$	-5.1 ± 0.2	8.7 ± 0.1	$26.1 \pm 0.0^*$	$1204 \pm 0.0^*$
R1.0	20.8 ± 0.2	18.4 ± 0.0	33.1 ± 0.1	85.9 ± 0.4	30.5 ± 0.3	14.5 ± 0.1	82.9 ± 0.3	1.4 ± 0.0	$-2.6 \pm 0.0^*$	8.9 ± 0.1	22.4 ± 0.3	986.9 ± 0.0
R1.5	18.3 ± 0.2	15.7 ± 0.1	29.2 ± 0.2	89.6 ± 0.1	28.3 ± 0.2	16.3 ± 0.1	82.5 ± 0.1	1.5 ± 0.1	-3.3 ± 0.0	9.1 ± 0.2	21.1 ± 0.3	868.4 ± 0.3
R2.0	15.5 ± 0.2	14.5 ± 0.1	26.5 ± 0.2	93.7 ± 0.1	23.7 ± 0.1	$19.8 \pm 0.0^*$	82.1 ± 0.1	1.6 ± 0.0	-3.5 ± 0.0	$9.5 \pm 0.2^*$	19.5 ± 0.1	644.4 ± 0.6

^a MC-moisture content, SC-swelling capacity, TS-tensile strength, EAB-elongation at break, OTR-oxygen transmission rate, WVTR-water vapour transmission rate. Data reported are mean \pm standard deviation and significant differences ($p < 0.05$) between different films. R0.0-control, R1.0-1% REO, R1.5-1.5% REO, R2.0-2% REO.



swelling capacity (18.4 to 14.1%) with the increased concentration of REO (Table 2).

The observed changes in hydration properties could be attributed to the increased hydrophobicity imparted by REO, along with the limited availability of hydroxyl groups in the biopolymers.²⁷ Comparable results were reported for sodium alginate films containing 2% laurel leaf extract, where the effect was linked to the presence of phenolic compounds in the extract.²⁸ Similarly, the water solubility reduced with increased concentration of REO with control having 41.2% and REO 2.0 with 26.5% solubility respectively (Table 2). This reduction may be due to polysaccharide–protein–phenolic interactions in the film matrix, that lowered the availability of hydroxyl and amino groups capable of interacting with water.²⁹ The presence of REO weakened the interaction between the water molecules and the film matrix.

3.1.2 Thickness and mechanical properties. The bionanocomposite film thickness ranged between 80.6 and 93.7 μm , with increasing REO concentrations resulting in thicker films (Table 2). The thickness of R2.0 film increased by 14% ($p < 0.05$). This may be due to the ability of REO droplets to fill the network of the film and act as film fillers. The tensile strength and elongation at break measurements of the film samples are presented in Table 2. The addition of REO (2%) led to a significant decrease in tensile strength (23.7 MPa) and a corresponding increase in elongation at break (19.8%) relative to the control films. This reduction in strength, coupled with enhanced extensibility, can be attributed to the structural discontinuities introduced by REO, which disrupted the continuity of the polymeric network. These findings are in agreement with other oil-incorporated biopolymer systems. For instance, polylactic acid/polybutylene adipate-*co*-terephthalate films with eucalyptus oil showed a 17% reduction in tensile strength relative to control films,³⁰ while starch–olive oil films exhibited a marked decrease from 21.95 MPa to 10.57 MPa.³¹ Compared to these composite biopolymer films, the developed C/SP/NC/REO(2%) films demonstrated comparatively higher mechanical integrity, with tensile strength values surpassing those reported for other biopolymer–oil combinations.³² Also C/NC/SP/REO films exhibited similar range of tensile strength when compared to conventional thermoplastics such as linear low density polyethylene, (17 MPa), polystyrene (22 MPa), high density polyethylene (28 MPa) respectively. This similarity in mechanical performance highlights their potential as viable alternatives to traditional petroleum-derived plastics.³³ Though the elongation at break of C/SP/NC/REO films was like that of polystyrene (11–20%) and lower than that of low-density polyethylene, their flexibility was sufficient for applications such as overwraps and laminate layers for paneer packaging.

3.1.3 Optical properties of the films. The color and opacity parameters of the bionanocomposite film are presented in Table 2. The transparency of the control film decreased, and yellowness of the film increased with the increase in REO concentration. The control films (R0.0) had an opacity of 8.7 A mm^{-1} , and it increased with the incorporation of essential oil, with R2.0 having highest opacity (9.5 A mm^{-1}). The oil droplets in the matrix enhanced the opacity by scattering light action.³⁴ The L^* , a^* , b^* and ΔE of the films were determined. The

incorporation of REO significantly ($p < 0.05$) increased the b^* values from -2.6 to -3.5 , while decreased the L^* and a^* values from 82.9 to 82.1 and 1.4 to 1.6, respectively, indicating a trend towards darkness and yellowness. The ΔE values showed an increase with the increase in REO content, implicating that REO had a high effect on the intrinsic yellow color of the film. The REO has good light barrier capability possibly due to the UV absorption ability of phenolic compounds in essential oils.^{34,35} Similar phenomena were observed in previous study with coffee oil.³⁶ Since REO droplets reduced the light transmittance specifically in the UV region, these may have potential application in extending the shelf-life of the UV sensitive foods.

3.1.4 WVTR and OTR. Table 2 shows the effects of REO and film matrix components on the water vapor transmission rate (WVTR) and oxygen transmission rate (OTR). The WVTR of the control film (R0.0) was highest ($1204 \text{ g m}^{-2} 24 \text{ h}^{-1}$), while the inclusion of REO progressively reduced the WVTR, with the lowest value observed in R2.0 films ($644.4 \text{ g m}^{-2} 24 \text{ h}^{-1}$). The addition of hydrophobic essential oil increased the tortuosity of the diffusion pathway, forcing water molecules to move through a more complex zigzag pattern, thereby lowering WVTR.³⁷ The microporous nature of the film, contributed by the hydrophobic oil agglomerates, further restricted the movement of water molecules in the films.

The OTR of R0.0 film ($26.1 \text{ cm}^{-2} 24 \text{ h}^{-1}$) reduced to $19.5 \text{ cm}^{-2} 24 \text{ h}^{-1}$ with the addition of 2% REO. The hydrophobic components may promote the polymer chain relaxation and cause interfacial debonding within the matrix, thereby increasing the pathways available for gas penetration through the film.³⁸ Similar studies of the incorporation of titanium oxide nanoparticles into the carboxymethylcellulose/arabic gum/gelatin matrix reduced the WVTR from 1236 to 1116 $\text{g m}^{-2} 24 \text{ h}^{-1}$ and the OTR from 40.34 to 27.97 $\text{cm}^{-2} 24 \text{ h}^{-1}$. The obstructive paths might form longer route for the transfer of water vapor molecules and oxygen gas, and lower the WVTR and OTR.³⁹

3.1.5 Structural characterization of the films. The crystalline features of bionanocomposite films were examined by XRD (Fig. 1). The XRD patterns of R0.0 films exhibited two main diffraction peaks at $2\theta = 23^\circ$ and 31.4° indicating crystalline nature. The diffractograms of carrageenan exhibited a broad hump in the range of 10 – 25° , indicating semi crystalline nature,⁴⁰ while soy protein showed a broad peak at 2θ (21.8°), indicating that amorphous globulin (7S and 11S).⁴¹

The diffractograms of nanocellulose had peaks with an intensity of 19.1° and 26.5° as reported in the International Centre for Diffraction Data (ICDD PDF no. 00-056-1718), contributing to the overall crystallinity of the films.⁴²

The addition of REO (1%, 1.5% and 2%) to the biopolymer films showed variation in the intensities of the major diffraction peaks (23° , 23.3° and 23.9° , respectively) emphasizing the alteration in the crystallinity of the film.²⁷ The presence of REO exhibited an amorphous film and the REO content possibly interferes with the hydrogen bond formation, resulting in compactness and reduction in film crystallinity. Similar variation in peak intensity has been reported for sodium alginate/casein films incorporated with different concentrations of orange oil.⁴³ Moreover, the observed changes in the mechanical



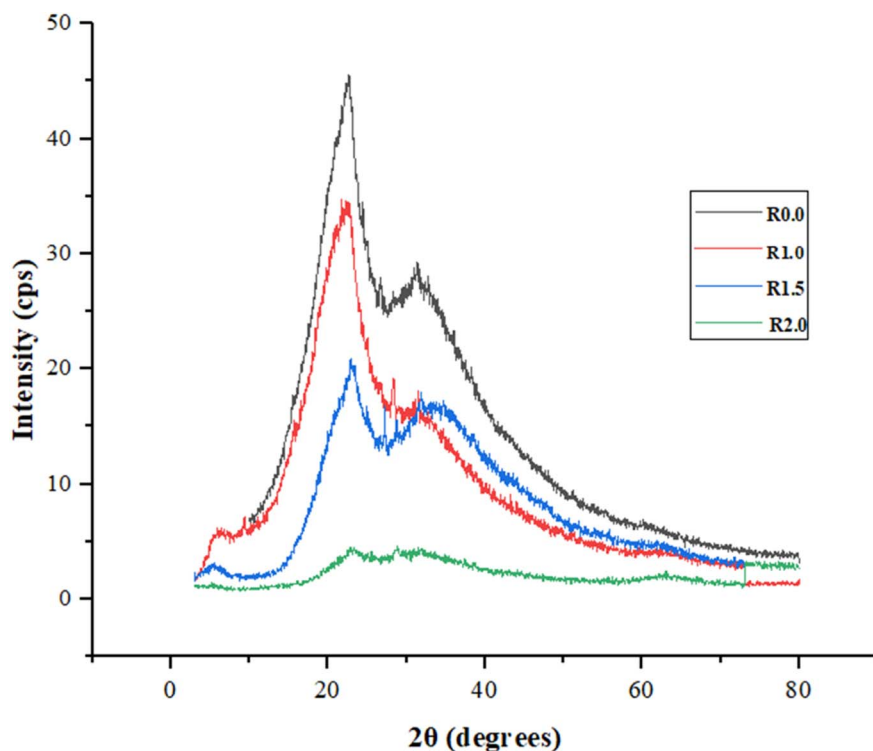


Fig. 1 X-ray diffraction studies of carrageenan-soy protein-nanocellulose-based bionanocomposite film incorporated with rosemary essential oil (REO). R0.0-control, R1.0-1% REO, R1.5-1.5% REO, R2.0-2% REO.

properties of the films may be attributed to these alterations in crystallinity resulting from compositional variations.

Fourier Transform Infrared Spectroscopy (FTIR) was used to monitor the association among the matrix constituents,

carrageenan, soy protein, nanocellulose and REO, that directly influence the physicochemical properties of the films. The broad-strong bands were observed between $3300\text{--}3600\text{ cm}^{-1}$ indicating --OH stretching possibly from carrageenan,

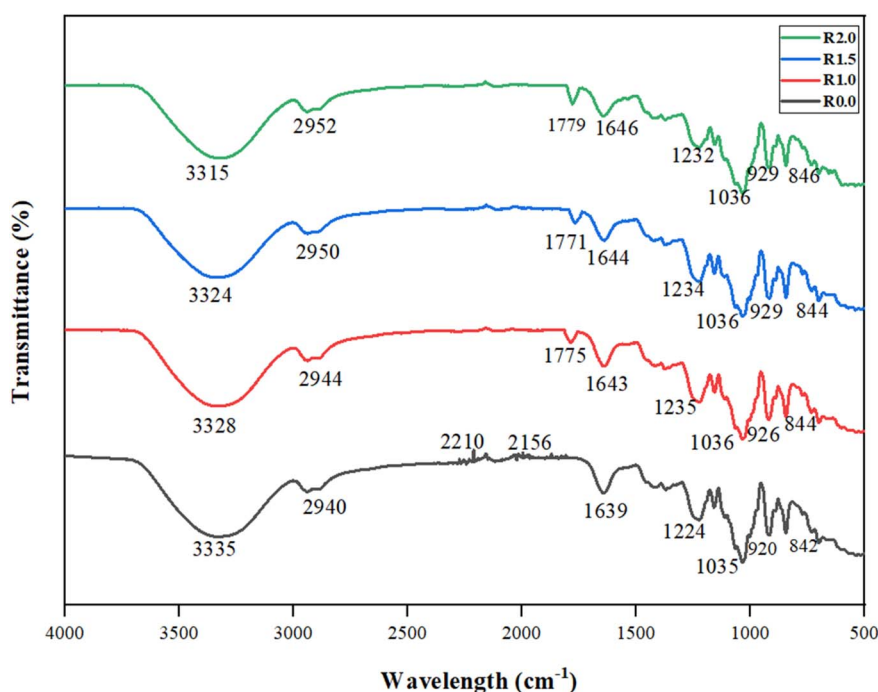


Fig. 2 FTIR images of carrageenan-soy protein-nanocellulose-based composite film incorporated with rosemary essential oil. R0.0-control, R1.0-1% REO, R1.5-1.5% REO, R2.0-2% REO.



nanocellulose and soy protein. The peaks in the range of 2940–2952 cm^{-1} were associated with C–H stretching vibrations, characteristic of carrageenan polymer chains. The absorption band observed at 2956 cm^{-1} is due to the C=C–C ring vibration of the volatile compounds in the REO.⁴⁴ The typical amide peak at 1639–1646 cm^{-1} represents the carbonyl group (amide I) and N–H stretching vibrations. Additionally, distinctive peaks at 920–929 cm^{-1} and 842–846 cm^{-1} were attributed to 3,6-anhydro-D-galactose and the C–O–SO₃ group of D-galactose-4-sulfate, respectively (Fig. 2). The variations in the absorption peaks intensity were likely due to overlapping chemical bond absorptions, suggesting strong and consistent interactions among the components.⁴⁵ Furthermore, the intermolecular hydrogen bonding strengthens the matrix and beneficially enhances the physical performance of the film. The control films displayed a prominent alkyne peak at 2210 cm^{-1} (–C≡C–), which diminished upon the incorporation of REO indicating high interactions between the REO and the other components of the film matrix. The shifts in the position and intensity of certain peaks after REO addition also emphasized the interactions between the functional groups of the essential oil and the –NH₂/–OH groups of the biopolymer matrix, indicating good miscibility (Table 3).

3.1.6 SEM and AFM. The SEM analysis was performed to gain deeper insight into the surface morphology of the bionanocomposite films, revealing key details about their surface characteristics and overall composition (Fig. 3a). The control biopolymer films exhibited a smooth, continuous, dense, and uniform morphology; however, the incorporation of REO (1–2%) increased the surface roughness of the films. Similar morphological changes have been reported earlier, where the behavior of the films was attributed to bubble-like oil droplet formation in the polysaccharide matrix, caused by the traction forces exerted during the evaporation process.⁴⁶ The presence of pores may also enhance the gas permeability of the films.

The topography of the bionanocomposite films were analyzed by atomic force microscopy (AFM). The bright peaks represent elevated position, while dark depressions correspond to lower positions on the films. The presence of both bright and dark areas on the bionanocomposite films indicate successful loading of REO. The roughness index of R0.0 films increased progressively with the increase in the concentration of REO. The surface roughness value, R_a and R_q of the R0.0 films was found

to be 3.29 and 2.66 nm. The REO (1%, 1.5% and 2%) incorporated films had R_a value 4.5 nm, 5.2 nm and 12.1 nm while R_q as 3.6, 3.9 and 8.1 nm, respectively; thus, revealing the rough topography with increase in R_a from 4.5 nm to 12.1 nm (Fig. 3b). Similar results of greater roughness were obtained in cassava starch-based films with the addition of geranium essential oil. The roughness and the surface irregularity are attributed by the presence of oil droplets accumulation during drying.⁴⁷

3.1.7 Water contact angle. The water resistance of bionanocomposite films is a critical factor for their practical applications. The WCA indicates the water sensitivity of the film surface. In general, films with a water contact angle greater than 65° are considered hydrophobic, whereas those with a water contact angle below 65° are classified as hydrophilic.⁴² The control films showed lowest WCA (98°), consistent with its hydrophilic properties. The addition of REO, significantly ($p < 0.05$) increased the WCA (106°, 107° and 109° for 1%, 1.5% and 2% REO) indicating surface hydrophobicity, weakening of the interactions between water molecules and hydrophilic groups of the films.⁴⁷ Similar trend was observed for the clove oil (10 wt%) and thyme oil (5 wt%) incorporated films, where the hydrophobicity increased from 72° to 80° and 62° to 74°, respectively.³⁰ The results emphasize the synergistic action of REO and matrix components in improving the hydrophobicity of the films. However, the high overall solubility of the films reflects the bulk composition of the matrix, which is dominated by hydrophilic biopolymers such as carrageenan and soy protein. Thus, while the film surface becomes less wettable, the internal polymer network remains susceptible to water penetration and dissolution. Practically, the short-term surface resistance to wetting is achieved due to the hydrophobic REO-rich surface, whereas the long-term water stability remains limited because of the hydrophilic nature of the bulk biopolymer matrix. This highlights the suitability of these films for packaging semi-moist or refrigerated foods, including paneer, where short-to medium-term moisture resistance is critical, rather than for high-humidity or liquid food applications (Fig. 4).

3.1.8 Thermal properties. The thermal stability of the bionanocomposite film containing REO was assessed using thermogravimetric analysis (TGA) and differential scanning calorimetry (DSC) which are important techniques for characterizing thermal behavior and degradation patterns (Fig. 5a).

Table 3 FTIR data of carrageenan-soy protein-nanocellulose-based composite film incorporated with rosemary essential oil. R0.0-control, R1.0-1% REO, R1.5-1.5% REO, R2.0-2% REO

Functional groups frequency range (cm^{-1})	Peak intensity (cm^{-1})				Reference group
	R0.0	R1.0	R1.5	R2.0	
3200–3600	3335	3340	3338	3331	O–H (hydroxyl)
2850–2960	2940	2944	2950	2952	C–H (alkane)
1640–1550	1639	1643	1644	1646	N–H (amide I)
1224–1235	1224	1235	1234	1232	C–H (alkane)
1029–1036	1035	1036	1036	1036	C–O and C–C
920–947	920	926	929	929	S=O (ester)
817–846	842	844	844	846	C–O–C (glycosidic linkage)



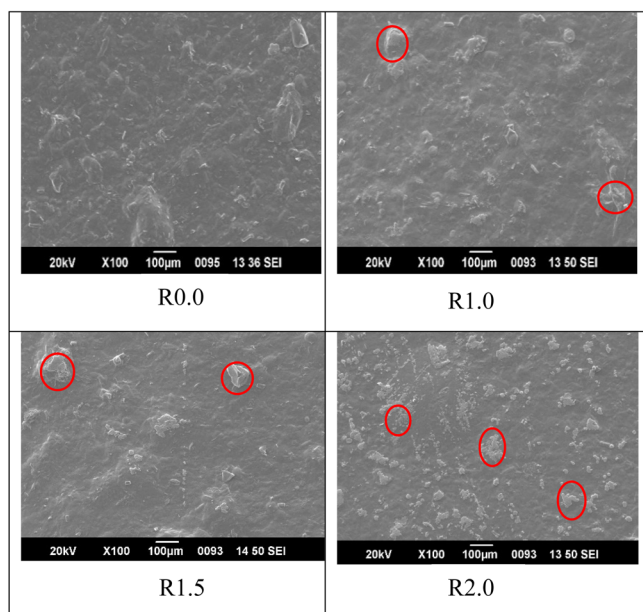


Fig. 3 (a)

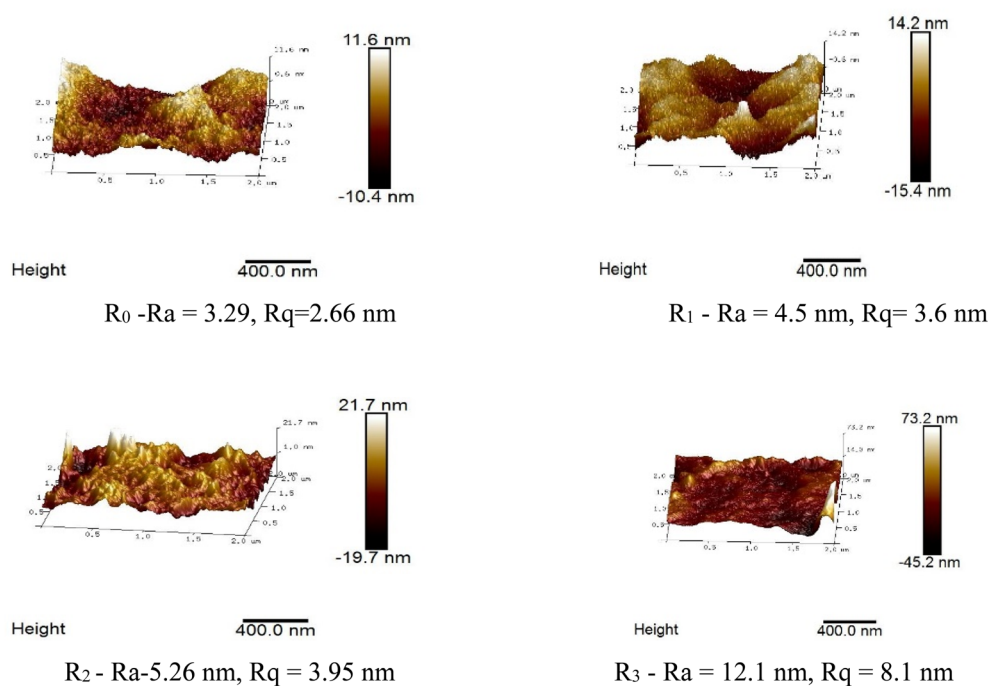


Fig. 3 (b)

Fig. 3 (a) SEM and (b) AFM images of carrageenan-soy protein-nanocellulose-based bionanocomposite film incorporated with rosemary essential oil REO based films. R0.0-control, R1.0-1% REO, R1.5-1.5% REO, R2.0-2% REO.

The films exhibited three main stages of weight loss. At the first stage (40–150 °C), all films lost approximately 12–14% of the original weight, primarily due to the evaporation of free and bound water as well as other volatile components. The oil incorporated films showed lesser weight loss, indicating reduced water absorption in the matrix due to their higher

hydrophobicity. The second stage of weight loss (139–300 °C), corresponding to 36–47% of the weight, was associated with the breakdown of polymer chains and the residual aromatic compounds from the essential oil.⁴⁸ The third weight loss stage (300–600 °C) involved disintegration of remaining film matrix. Similar studies on the incorporation of cellulose nanocrystals



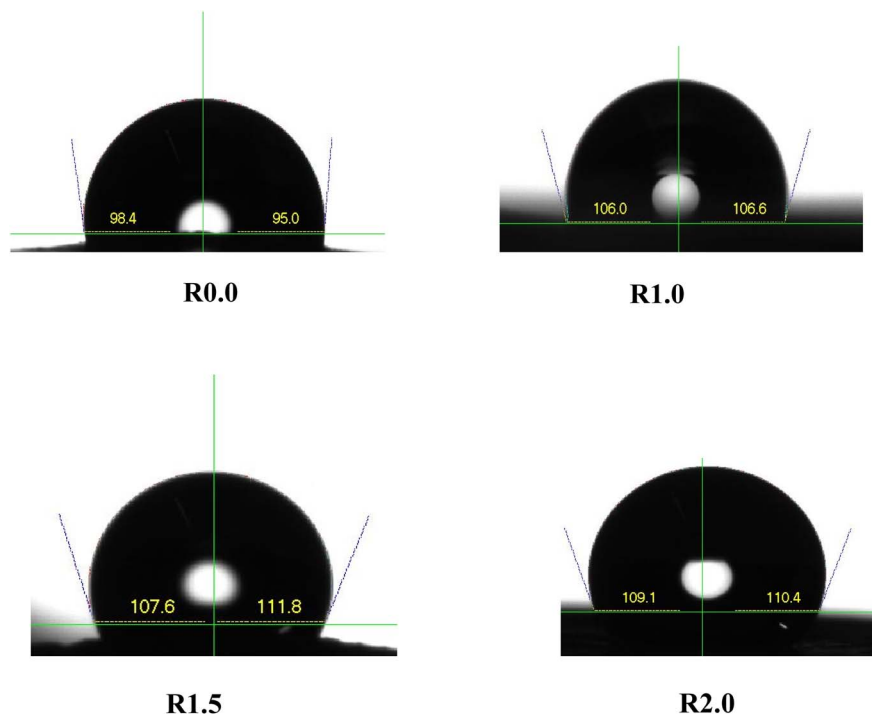


Fig. 4 Contact angle images of carrageenan-soy protein-nanocellulose-based bionanocomposite film incorporated with rosemary essential oil. R0.0-control, R1.0-1% REO, R1.5-1.5% REO, R2.0-2% REO.

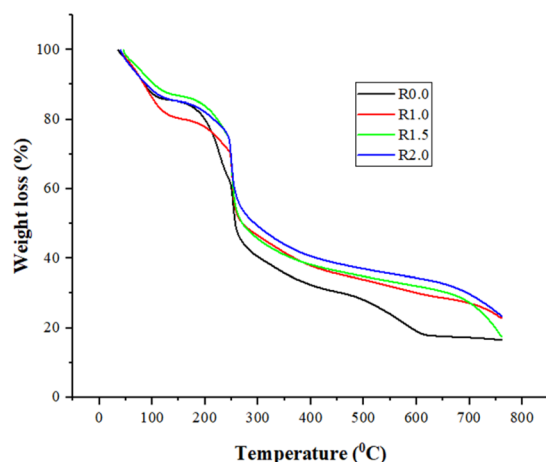


Fig. 5 (a)

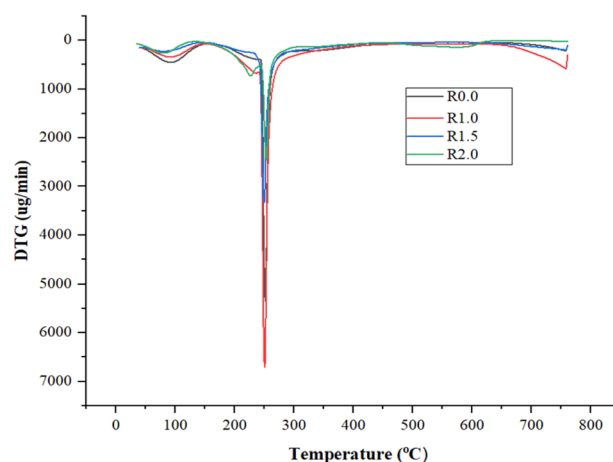


Fig. 5 (b)

Fig. 5 (a) TGA and (b) DSC graphs of carrageenan-soy protein-nanocellulose based bionanocomposite film incorporated with rosemary essential oil R0.0-control, R1.0-1% REO, R1.5-1.5% REO, R2.0-2% REO.

into alginate-based films enhanced their thermal stability.⁴⁹ The films with higher concentrations of REO showed increased thermal degradation, due to the volatile properties of the oil and its plasticizing effect. The DSC graphs for the bionanocomposite films are represented in Fig. 5b. The melting temperature showed a shift with the addition of REO and R2.0 composite film had the high melting temperature (253 °C) compared to the control films, which may be attributed due to

the crosslinking of the polyphenolic constituents in oil with matrix components.²⁷

3.1.9 Antimicrobial and antioxidant properties. The agar disc diffusion method was employed to evaluate the antimicrobial activity against the Gram positive and Gram-negative bacteria. The incorporation of REO (2%) showed significantly ($p < 0.05$) higher antibacterial activity against *Bacillus cereus* (25 mm), followed by *Staphylococcus aureus* (19 mm), *E. coli* (18 mm)



and *Salmonella typhi* (17 mm) (Table 3). The inhibitory effect against *Bacillus cereus* may be attributed to the gradual release of hydrophobic molecules from REO incorporated in the films, as the teichoic and lipoteichoic acids present in the bacterial cell wall can facilitate the attachment and penetration of lipid components into the microbial cell membrane, thereby increasing its permeability and result in cell death.⁵⁰ The reduced inhibition observed in *Salmonella typhi* could be linked to the presence of lipopolysaccharides in the outer membrane that act as a barrier, limiting the movement of hydrophobic compounds through the polysaccharide layer. The more complex lipopolysaccharide structure with elaborate O-antigen chains of the Gram-negative bacteria, *Salmonella typhi* functions as an effective barrier that limits the diffusion of antibacterial agents. The effect of essential oil in *Salmonella typhi* is largely restricted to its outer membrane (lipopolysaccharide layer) where the hydrophobic essential oil components embed themselves by disrupting the structural arrangement of the membrane but restrict them from diffusing into the cytoplasm. Thus, the Gram-negative bacteria exhibit greater resistance to essential oils compared to Gram-positive bacteria, mainly due to differences in their membrane structure which act as a barrier and restrict diffusion of antibacterial agents.⁵¹ Similar studies in agar cellulose bionanocomposite film with savory essential oil exhibited reduced antimicrobial activity in Gram negative bacteria which was attributed due to the presence of lipopolysaccharides in the cell wall of Gram-negative bacteria, which act as a barrier and restrict the penetration of essential oil components into the cytoplasmic membrane.⁵² When compared with other essential oils, including tea tree, thyme, wild orange, peppermint, lemon, clove, and cinnamon,

rosemary oil demonstrated the highest antimicrobial efficacy and was identified as the most effective broad-spectrum antibacterial agent.⁵³


The assessment of antioxidant activity is crucial for evaluating the performance of active packaging. The DPPH antioxidant capacity of the films are displayed in Table 4. The antioxidant property of the bionanocomposite films was enhanced with the increased concentration of REO (IC_{50} -0.61, 0.35 and 0.24 mg mL⁻¹ for 1, 1.5 and 2% REO, respectively). This could be due to the hydroxyl groups of the polyphenols and flavonoids attached to the aromatic rings that facilitate hydrogen/electron donation to free radicals.⁵⁴ Similar findings of higher DPPH activity of 50% was observed in chitosan films with thymus essential oil, compared to control films without essential oil (2%).⁵⁵

3.1.10 Biodegradability study. The soil burial test was conducted on a laboratory scale under controlled environment. During the test, soil moisture readily penetrated the polymer network, disrupting the polymer chains and making them more susceptible to biodegradation by soil microorganisms, thereby accelerating the degradation rate.⁵⁶ The biodegradation rate of the films over time was indicated by weight loss (Fig. 6). After 28 days, bionanocomposite films with 2% REO showed slight reduction in the degradation (90%) than control films (96%), which may be due to the hydrophilic nature of latter.⁵⁷ Similar findings were recorded for the thermoplastic starch films incorporated with pectin and lemon grass oil that degraded within 20 days during soil burial test.

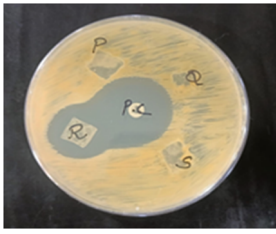
3.1.11 Preservation performance of paneer. The application of bionanocomposite films as active packaging solutions for the extension of shelf life of paneer under refrigeration was


Table 4 Antimicrobial and antioxidant activity of carrageenan-soy protein-nanocellulose-based bionanocomposite film incorporated with rosemary essential oil^a


Sample	Zone of inhibition			
	<i>B. cereus</i>	<i>S. aureus</i>	<i>E. coli</i>	<i>S. typhi</i>
Gentamycin	32 ± 0.2*	28 ± 0.2*	25 ± 0.3*	27 ± 0.2*
R0.0	ND	ND	ND	ND
R1.0	ND	ND	ND	ND
R1.5	ND	ND	ND	ND
R2.0	25 ± 0.1	19 ± 0.2	18 ± 0.1	17 ± 0.2



Inhibition zone (R2.0)







Antioxidant activity of C/SP/NC incorporated REO nanocomposite films				
DPPH IC_{50} (mg mL ⁻¹)	R0.0	R1.0	R1.5	R2.0
	3.80 ± 0.0*	0.61 ± 0.0	0.35 ± 0.0	0.24 ± 0.0

^a PC-positive control (Gentamycin), ND-not detected. R0.0-control, R1.0-1% REO, R1.5-1.5% REO, R2.0-2% REO. Data reported are mean ± standard deviation and significant differences ($p < 0.05$) between different films.



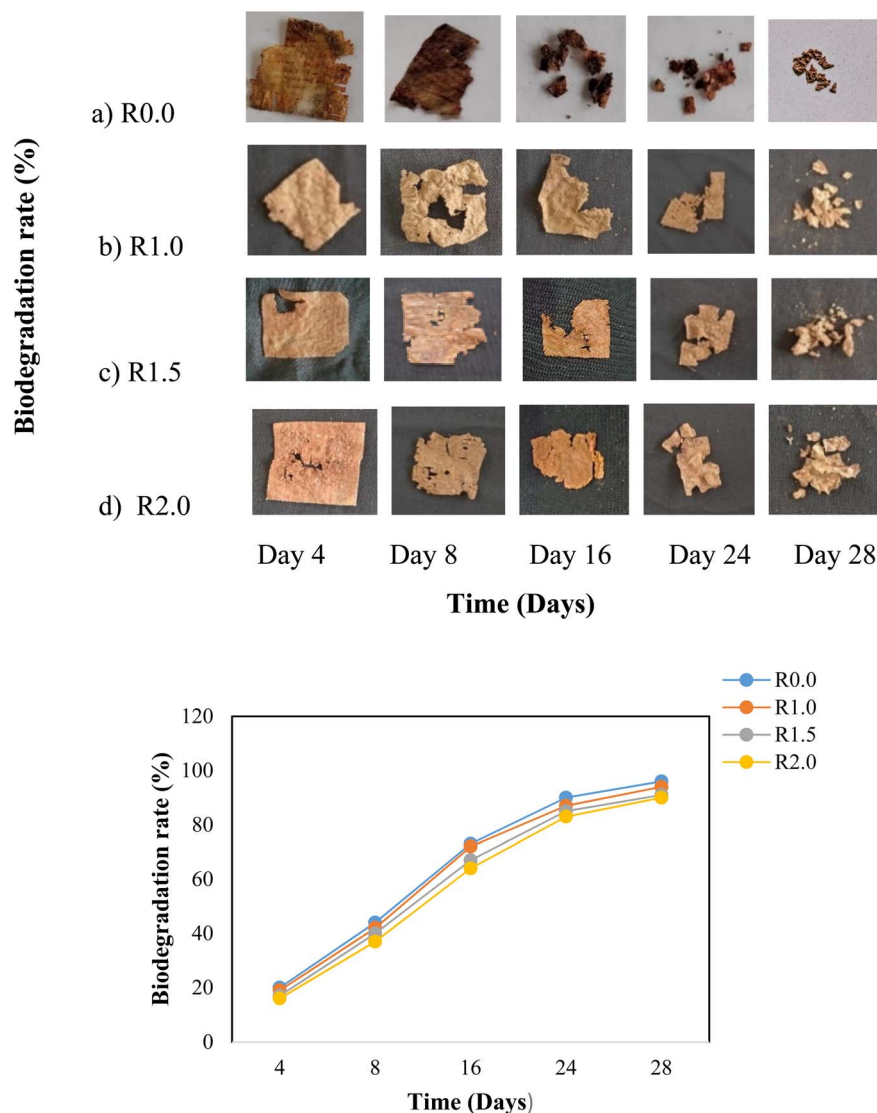


Fig. 6 Biodegradation rate of carrageenan-soy protein-nanocellulose based bionanocomposite film incorporated with rosemary essential oil. R0.0-control, R1.0-1% REO, R1.5-1.5% REO, R2.0-2% REO.

carried out and the results of physicochemical and textural changes are represented in Table 5. The amount of moisture content in paneer showed a gradual decrease with increased storage period (from 55.0 to 42.8%, after 28 days) for R2.0 films (from 55.0 to 45.1% in 10 days). Similar results were recorded where the maximum weight loss up to 55% was observed in paneer samples which was untreated compared to copper nanoparticles coated paneer, after 14 days of refrigerated storage.⁵⁸ The titratable acidity showed an increased from 0.35 (control) to 0.8 (R0.0 after 10 days) and 0.76% (R2.0 films after 28 days). These variations in the titratable acidity may be attributed to the microbial fermentation and accumulation of the metabolic products. The tyrosine content indicating the protein breakdown due to autolysis and bacterial activity, increased with storage time. The tyrosine value varied from 5.2 to 23.3 mg/100 g of tyrosine for R2.0 films after 28 days. The proteolysis was estimated to be minimum in oil incorporated

films than R0.0 films (6.9 to 19.5 mg/100 g after 10 days). Similar outcomes were obtained for paneer wrapped in chitosan and clove essential oil-based films.⁵⁹ The color parameters (L^* , a^* and b^* value) that significantly influence consumer acceptance showed a considerable deviation ($p < 0.05$). The lightness value (L^*) of paneer was found to reduce with the increase in storage time with L^* value 85.2 to 79.8 (10 days) and 88.1 to 75.2 (28 days) for R0.0 and R2.0 films. Similar patterns were observed for a^* and b^* values.

The hardness was estimated to be 54.7 and 69 N after 10 and 28 days for R0.0 and R2.0, respectively, which may be attributed to the structural disintegration of proteins, and the amount of dry matter content, both of which affected the chewiness and gumminess of paneer. The chewiness value was observed to increase with the extension of storage period. The chewiness of paneer (R2.0) was found to be 9.8 N after 28 days of storage. Similar results were reported for paneer under refrigerated



Table 5 Shelf-life studies of carrageenan-soy protein-nanocellulose bionanocomposite film in refrigerated storage (4 °C)

Films	Storage days	Moisture content (%)	Titratable acidity (%)	Tyrosine (mg/100 g)	Colour			Hardness (N)	Chewiness (N)
					<i>L</i> *	<i>a</i> *	<i>b</i> *		
(a) R0.0-control films									
R0.0	0	55.0 ± 0.0	0.3 ± 0.0	6.9 ± 0.1*	85.2 ± 0.0	1.4 ± 0.0*	15.4 ± 0.1*	37.2 ± 0.1 ^a	1.8 ± 0.0 ^a
	1	53.3 ± 0.1	0.5 ± 0.0	8.5 ± 0.0*	84.7 ± 0.0	1.9 ± 0.0*	15.7 ± 0.1*	39.3 ± 0.1 ^a	2.5 ± 0.0 ^a
	3	48.2 ± 0.1	0.6 ± 0.0	10.3 ± 0.0	83.4 ± 0.0	2.1 ± 0.0	16.4 ± 0.0*	45.0 ± 0.0	4.9 ± 0.1
	7	47.2 ± 0.0	0.7 ± 0.0	16.1 ± 0.0*	80.1 ± 0.0	2.8 ± 0.0*	16.9 ± 0.0	49.0 ± 0.0*	7.4 ± 0.1*
	10	45.1 ± 0.1	0.8 ± 0.1	19.5 ± 0.1*	79.8 ± 0.0	3.3 ± 0.0*	17.7 ± 0.0*	54.7 ± 0.0*	8.1 ± 0.0*
(b) R2.0-2% REO films									
R2.0	0	55.2 ± 0.1*	0.36 ± 0.0	5.2 ± 0.0	88.1 ± 0.0*	0.8 ± 0.0	15.0 ± 0.0	33.3 ± 0.0	1.4 ± 0.1
	1	54.7 ± 0.0 ^a	0.41 ± 0.0	5.5 ± 0.0	89.7 ± 0.0	0.9 ± 0.1	15.2 ± 0.0	35.7 ± 0.2	3.3 ± 0.1
	4	54.1 ± 0.1	0.53 ± 0.0	6.5 ± 0.0	86.5 ± 0.0*	1.1 ± 0.1	15.4 ± 0.0	43.2 ± 0.2	3.6 ± 0.0
	7	52.4 ± 0.1*	0.55 ± 0.1	7.1 ± 0.0	85.0 ± 0.1*	1.2 ± 0.0	16.2 ± 0.0	48.3 ± 0.1	4.3 ± 0.0
	10	50.9 ± 0.0*	0.57 ± 0.0	8.7 ± 0.0	83.4 ± 0.0*	1.4 ± 0.0	16.8 ± 0.0	52.1 ± 0.1	5.0 ± 0.1
	13	49.7 ± 0.0	0.59 ± 0.0	9.9 ± 0.0	83.2 ± 0.0	2.0 ± 0.0	17.6 ± 0.0	55.8 ± 0.1	6.3 ± 0.1
	16	48.8 ± 0.0	0.61 ± 0.0	11.6 ± 0.0	82.6 ± 0.0	2.3 ± 0.0	17.7 ± 0.0	59.1 ± 0.0	6.7 ± 0.0
	19	46.0 ± 0.0	0.66 ± 0.0	13.7 ± 0.0	81.6 ± 0.0	2.6 ± 0.0	17.9 ± 0.0	61.8 ± 0.1	7.7 ± 0.0
	22	45.8 ± 0.0	0.70 ± 0.0	15.4 ± 0.1	80.2 ± 0.0	2.8 ± 0.0	18.3 ± 0.0	63.8 ± 0.1	8.3 ± 0.0
	25	43.6 ± 0.0	0.72 ± 0.0	18.1 ± 0.1	78.7 ± 0.1	3.2 ± 0.0	18.5 ± 0.0	68.3 ± 0.1	8.7 ± 0.0
	28	42.8 ± 0.1	0.76 ± 0.0	23.3 ± 0.1	75.2 ± 0.1	3.5 ± 0.0	19.2 ± 0.0	69.2 ± 0.2	9.8 ± 0.0

^a Data reported are mean ± standard deviation and significant differences ($P < 0.05$) are estimated between different samples.

storage.⁵² Thus, the shelf life of the paneer packed in bionanocomposite films extended its shelf life to 28 days.

The C/SP/NC bionanocomposite films were effective in maintaining the storage stability of paneer under refrigeration for up to 28 days. However, the primary limitations observed were related to the hardness and color parameters of the paneer. Beyond this period, further extension of shelf life appears feasible, provided strategies are developed to address these quality attributes. Further research can be carried out to enhance shelf life, improve quality of food stored in bionanocomposite films. Moreover, improving the industrial scalability of such bionanocomposite films will be critical, which could be achieved through advanced fabrication techniques such as extrusion and electrospinning, coupled with cost-effective local manufacturing approaches. These include the difficulty of achieving uniform nanofiller dispersion at high production volumes, variability in mechanical and barrier properties between batches, and the limited compatibility of novel films with conventional food processing and packaging machinery. Furthermore, the energy-intensive nature of certain fabrication processes restricts large-scale adoption, particularly in resource-limited settings. The development of cost-effective, locally adaptable manufacturing strategies and optimizing processing conditions to reduce energy inputs will therefore be crucial for successful commercialization. Furthermore, scalable and eco-friendly strategies for incorporating smart functionalities such as low-cost film formulation technologies remain insufficiently explored. In parallel, the integration of emerging intelligent packaging systems, such as pH-sensitive indicators and controlled release of antimicrobial agents, offers a promising pathway for enhancing product shelf life, ensuring consistent quality and ultimately increasing the marketability

of paneer and other perishable foods. Overcoming these gaps will require interdisciplinary efforts that bridge material science, food technology and regulatory frameworks, ensuring that bionanocomposite films are economically viable, environmentally sustainable, and socially acceptable.

Conclusion

The current study revealed that the incorporation of rosemary essential oil (REO) in the carrageenan/soy protein/nanocellulose films produced thicker films (85.9–93.7 μm) with lesser water solubility (33.1–26.5%). Additionally, the presence of 2% REO resulted in the reduction in water vapour and oxygen transmission rate to 644.4 g m⁻².24 h and 19.5 cm⁻² 24 h⁻¹ with the increase in percent elongation (19.8%) of the films. The FTIR spectra of the composite films showed no significant changes. Furthermore, the addition of REO improved the antioxidant properties and the film showed higher zone of inhibition of 19 mm and 25 mm against the Gram-positive bacteria (*Staphylococcus aureus* and *Bacillus cereus*). The degradability of the films in soil was estimated to be 90% after 28 days which offers a promising pathway towards sustainability and foster a greener future. The storage studies of paneer in the bionanocomposite films at refrigerated condition (4 °C) indicated shelf life of 28 days with minimum changes in its textural parameters along with titratable acidity (0.76%) and tyrosine content (23.3 mg/100 g). The results suggested that the bionanocomposite films exhibited greater potential to be used as an active food packaging material. The observed shelf life of 28 days for paneer packed in bionanocomposite films is notably higher compared to only 10 days when packed in commercial films, highlighting the effectiveness of the developed packaging system in preserving



product quality. However, beyond 28 days of storage, noticeable changes were observed in the textural attribute of hardness and in the color of paneer, despite other physicochemical and microbiological parameters remaining within acceptable limits. These alterations may be attributed to possible interactions between rosemary oil and milk proteins, which could influence the structural integrity of the product. To overcome this limitation, future investigations should explore the use of familiar, consumer-accepted materials that can maintain shelf life without adversely affecting texture and sensory characteristics. Sensory studies in the later part of the study indicated hardened texture and browning of the paneer cubes, which are possibly attributed to the dehydration and migration of phenolics to paneer from the film. The future applied research may act on these and develop films to maintain the texture and structural integrity of the food. In this context, bilayer membranes, encapsulation could be chosen as future research areas.

The potential challenges in translating this work to a commercial scale include the variability in the purity of raw material batches, which may affect film quality and reproducibility. In addition, large-scale production requires equipment specifically designed to accommodate the characteristics of the raw materials and has several technical barriers. These include difficulties in producing continuous films, prolonged drying times, limited control over film thickness, high energy consumption, and elevated production costs. The addressing of these limitations is therefore essential for enabling industrial scalability. In this regard, future research should focus on developing specific optimized processing strategies, such as employing large pilot-scale casting units, cost-effective fabrication techniques that reduce energy consumption, production time, and material costs to address scalability and industrial feasibility challenges. Despite these challenges, the present study demonstrates a significant novelty by highlighting that a hybrid carrageenan soy protein matrix reinforced with nanocellulose and incorporated with rosemary essential oil can simultaneously enhance the mechanical strength, barrier properties, and antimicrobial activity of the films. Collectively, these findings contribute to advancing the development of multifunctional, biodegradable packaging materials with strong potential for food preservation applications.

Conflicts of interest

The authors declare that they have no known competing financial interests or personal ties that could appear to have influenced the work revealed in this paper.

Data availability

The data supporting the findings of this research are available in the article.

Acknowledgements

The authors thank Sophisticated Analytical Testing Facilities (SAIF) under Department of Science and Technology, Cochin,

for assistance with TGA, FTIR and SEM studies, Sophisticated Analytical Instrument Facility, (STIC) M G University for AFM and Central Institute of Plastic Engineering and Technology (CIPET) Kochi, for assistance with tensile strength, percent elongation and thickness.

References

- 1 J. Baranwal, B. Barse, A. Fais, G. L. Delogu and A. Kumar, Biopolymer: A sustainable material for food and medical applications, *Polymers*, 2022, **14**(5), 983, DOI: [10.3390/polym14050983](https://doi.org/10.3390/polym14050983).
- 2 X. Zhao, Y. Wang, X. Chen, X. Yu, W. Li, S. Zhang and H. Zhu, Sustainable bioplastics derived from renewable natural resources for food packaging, *Matter*, 2023, **6**(1), 97–127, DOI: [10.1016/j.matt.2022.11.007](https://doi.org/10.1016/j.matt.2022.11.007).
- 3 B. Deepa, E. Abraham, L. Pothan, N. Cordeiro, M. Faria and S. Thomas, Biodegradable nanocomposite films based on sodium alginate and cellulose nanofibrils, *Materials*, 2016, **9**, 50, DOI: [10.3390/ma9010050](https://doi.org/10.3390/ma9010050).
- 4 H. P. S. Abdul Khalil, Y. Y. Tye, C. Y. Kok and C. K. Saurabh, Preparation and characterization of modified and unmodified carrageenan-based films, *IOP Conf. Ser.: Mater. Sci. Eng.*, 2018, **368**, 012020, DOI: [10.1088/1757-899X/368/1/012020](https://doi.org/10.1088/1757-899X/368/1/012020).
- 5 P. Fathiraja, S. Gopalrajan, M. Karunanithi, M. Nagarajan, M. C. Obaiah, S. Durairaj and N. Neethirajan, Development of a biodegradable composite film from chitosan, agar and glycerol based on optimization process by response surface methodology, *Cellul. Chem. Technol.*, 2021, **55**(7–8), 849–865, DOI: [10.35812/CelluloseChemTechnol.2021.55.72](https://doi.org/10.35812/CelluloseChemTechnol.2021.55.72).
- 6 N. P. Risyon, S. H. Othman, R. K. Basha and R. A. Talib, Characterization of polylactic acid/halloysite nanotubes bionanocomposite films for food packaging, *Food Packag. Shelf Life*, 2020, **23**, 100450, DOI: [10.1016/j.fpsl.2019.100450](https://doi.org/10.1016/j.fpsl.2019.100450).
- 7 R. Chawla, S. Sivakumar and H. Kaur, Antimicrobial edible films in food packaging: Current scenario and recent nanotechnological advancements – a review, *Carbohydr. Polym. Technol. Appl.*, 2021, **2**, 100024, DOI: [10.1016/j.carpta.2021.100024](https://doi.org/10.1016/j.carpta.2021.100024).
- 8 S. Akhter, M. S. Jahan, M. L. Rahman, T. A. Ruhane, M. Ahmed and M. A. Khan, Revolutionizing sustainable fashion: Jute-mycelium vegan leather reinforced with polyhydroxyalkanoate biopolymer crosslinking from novel bacteria, *Adv. Polym. Technol.*, 2024, 1304800, DOI: [10.1155/2024/1304800](https://doi.org/10.1155/2024/1304800).
- 9 S. Kumar, D. C. Rai, K. Niranjana and Z. F. Bhat, Paneer—An Indian soft cheese variant: a review, *J. Food Sci. Technol.*, 2014, **51**, 821–831, DOI: [10.1007/s13197-011-0567-x](https://doi.org/10.1007/s13197-011-0567-x).
- 10 J. P. Maran, V. Sivakumar, K. Thirugnanasambandham and R. Sridhar, Microwave assisted extraction of pectin from waste *Citrullus lanatus* fruit rinds, *Carbohydr. Polym.*, 2014, **101**, 786–791, DOI: [10.1016/j.carbpol.2013.09.062](https://doi.org/10.1016/j.carbpol.2013.09.062).
- 11 Y. Walid, N. Malgorzata, R. Katarzyna, B. Piotr, O. L. Ewa, B. Izabela and S. T. Moufida, Effect of rosemary essential oil and ethanol extract on physicochemical and antibacterial properties of optimized gelatin–chitosan film



- using mixture design, *J. Food Process. Preserv.*, 2022, **46**(1), e16059, DOI: [10.1111/jfpp.16059](https://doi.org/10.1111/jfpp.16059).
- 12 S. Roy, S. Shankar and J. W. Rhim, Melanin-mediated synthesis of silver nanoparticle and its use for the preparation of carrageenan-based antibacterial films, *Food Hydrocolloids*, 2019, **88**, 237–246, DOI: [10.1016/j.foodhyd.2018.10.013](https://doi.org/10.1016/j.foodhyd.2018.10.013).
 - 13 A. Hadi, A. Nawab, F. Alam and S. Naqvi, Development of sodium alginate-aloe vera hydrogel films enriched with organic fibers: study of the physical, mechanical, and barrier properties for food-packaging applications, *Sustainable Food Technol.*, 2023, **1**(6), 863–873, DOI: [10.1039/D3FB00122A](https://doi.org/10.1039/D3FB00122A).
 - 14 H. Doh, Development of seaweed biodegradable nanocomposite films reinforced with cellulose nanocrystals for food packaging, Doctoral dissertation, Clemson University, 2020.
 - 15 S. Remya, C. O. Mohan, J. Bindu, G. K. Sivaraman, G. Venkateshwarlu and C. N. Ravishankar, Effect of chitosan based active packaging film on the keeping quality of chilled stored barracuda fish, *J. Food Sci. Technol.*, 2016, **53**, 685–693, DOI: [10.1007/s13197-015-2018-6](https://doi.org/10.1007/s13197-015-2018-6).
 - 16 S. R. Kanatt, Development of active/intelligent food packaging film containing *Amaranthus* leaf extract for shelf-life extension of chicken/fish during chilled storage, *Food Packag. Shelf Life*, 2020, **24**, 100506, DOI: [10.1016/j.fpsl.2020.100506](https://doi.org/10.1016/j.fpsl.2020.100506).
 - 17 B. B. Sedayu, M. J. Cran and S. W. Bigger, Reinforcement of refined and semi-refined carrageenan film with nanocellulose, *Polymers*, 2020, **12**(5), 1145, DOI: [10.3390/polym12051145](https://doi.org/10.3390/polym12051145).
 - 18 M. Azarifar, B. Ghanbarzadeh, M. S. Khiabani, A. A. Basti, A. Abdulkhani, N. Noshirvani and M. Hosseini, The optimization of gelatin-CMC based active films containing chitin nanofiber and *Trachyspermum ammi* essential oil by response surface methodology, *Carbohydr. Polym.*, 2019, **208**, 457–468, DOI: [10.1016/j.carbpol.2019.01.005](https://doi.org/10.1016/j.carbpol.2019.01.005).
 - 19 A. S. Abd, E. Elhafyan, A. R. Siddiqui, W. Alnoush, M. J. Blunt and N. Alyafei, A review of the phenomenon of counter-current spontaneous imbibition: Analysis and data interpretation, *J. Pet. Sci. Eng.*, 2019, **180**, 456–470, DOI: [10.1016/j.petrol.2019.05.066](https://doi.org/10.1016/j.petrol.2019.05.066).
 - 20 W. Yeddes, M. Nowacka, K. Rybak, I. Younes, M. Hammami, M. Saidani-Tounsi and D. Witrowa-Rajchert, Evaluation of the antioxidant and antimicrobial activity of rosemary essential oils as gelatin edible film component, *Food Sci. Technol. Res.*, 2019, **25**(2), 321–329, DOI: [10.3136/FSTR.25.321](https://doi.org/10.3136/FSTR.25.321).
 - 21 J. H. Li, J. Miao, J. L. Wu, S. F. Chen and Q. Q. Zhang, Preparation and characterization of active gelatin-based films incorporated with natural antioxidants, *Food Hydrocolloids*, 2014, **37**, 166–173, DOI: [10.1016/j.foodhyd.2013.10.015](https://doi.org/10.1016/j.foodhyd.2013.10.015).
 - 22 A. H. M. Zain, M. K. Ab Wahab and H. Ismail, Biodegradation behaviour of thermoplastic starch: the roles of carboxylic acids on cassava starch, *J. Polym. Environ.*, 2018, **26**, 691–700, DOI: [10.1007/s10924-017-0978-5](https://doi.org/10.1007/s10924-017-0978-5).
 - 23 AOAC International, *Official Methods of Analysis*, AOAC, 17th edn, 2000.
 - 24 S. B. Kumbhar, J. S. Ghosh and S. P. Samudre, Microbiological analysis of pathogenic organisms in indigenous fermented milk products, *Adv. J. Food Sci. Technol.*, 2009, **1**(1), 35–38.
 - 25 E. D. Strange, R. C. Benedict, J. L. Smith and C. E. Swift, Evaluation of rapid tests for monitoring alterations in meat quality during storage, *J. Food Prot.*, 1977, **40**(12), 843–847, DOI: [10.4315/0362-028X-40.12.843](https://doi.org/10.4315/0362-028X-40.12.843).
 - 26 T. J. Gutiérrez, N. J. Morales, E. Pérez, M. S. Tapia and L. Famá, Physico-chemical properties of edible films derived from native and phosphorylated yam and cassava starches, *Food Packag. Shelf Life*, 2015, **3**, 1–8, DOI: [10.1016/j.fpsl.2014.09.002](https://doi.org/10.1016/j.fpsl.2014.09.002).
 - 27 S. Bhatia, Y. Abbas Shah, A. Al-Harrasi, M. Jawad, E. Koca and L. Y. Aydemir, Enhancing tensile strength, thermal stability, and antioxidant characteristics of transparent kappa carrageenan films using grapefruit essential oil for food packaging applications, *ACS Omega*, 2024, **9**(8), 9003–9012, DOI: [10.1016/j.heliyon.2024.e36895](https://doi.org/10.1016/j.heliyon.2024.e36895).
 - 28 M. Moura-Alves, V. G. L. Souza, J. A. Silva, A. Esteves, L. M. Pastrana, C. Saraiva and M. A. Cerqueira, Characterization of sodium alginate-based films blended with olive leaf and laurel leaf extracts obtained by ultrasound-assisted technology, *Foods*, 2023, **12**(22), 4076, DOI: [10.3390/foods12224076](https://doi.org/10.3390/foods12224076).
 - 29 S. Sharma, S. Barkauskaite, S. Jaiswal, B. Duffy and A. K. Jaiswal, Development of essential oil incorporated active film based on biodegradable blends of poly(lactide)/poly(butylene adipate-co-terephthalate) for food packaging application, *J. Packag. Technol. Res.*, 2020, **4**(3), 235–245, DOI: [10.1007/s41783-020-00099-5](https://doi.org/10.1007/s41783-020-00099-5).
 - 30 T. Li, N. Xia, L. Xu, H. Zhang, H. Zhang, Y. Chi and H. Li, Preparation, characterization and application of SPI-based blend film with antioxidant activity, *Food Packag. Shelf Life*, 2021, **27**, 100614, DOI: [10.1016/j.fbio.2021.100927](https://doi.org/10.1016/j.fbio.2021.100927).
 - 31 Y. Li, C. Tang and Q. He, Effect of orange (*Citrus sinensis* L.) peel essential oil on characteristics of blend films based on chitosan and fish skin gelatin, *Food Biosci.*, 2021, **41**, 100927, DOI: [10.3389/fnut.2022.882742](https://doi.org/10.3389/fnut.2022.882742).
 - 32 R. Guesmi, N. Benbettaieb, M. R. Ben Romdhane, T. Barhoumi-Slimi and A. Assifaoui, In situ polymerization of linseed oil-based composite film: Enhancement of mechanical and water barrier properties by the incorporation of cinnamaldehyde and organoclay, *Molecules*, 2022, **27**(22), 8089, DOI: [10.3390/molecules27228089](https://doi.org/10.3390/molecules27228089).
 - 33 S. Shaikh, M. Yaqoob and P. Aggarwal, An overview of biodegradable packaging in food industry, *Curr. Res. Food Sci.*, 2021, **4**, 503–520.
 - 34 B. Wang, S. Yan, L. Qiu, W. Gao, X. Kang, B. Yu and A. M. Abd El-Aty, Antimicrobial activity, microstructure, mechanical, and barrier properties of cassava starch composite films



- supplemented with geranium essential oil, *Front. Nutr.*, 2022, **9**, 882742, DOI: [10.3389/fnut.2022.882742](https://doi.org/10.3389/fnut.2022.882742).
- 35 B. Wang, S. Yan, W. Gao, X. Kang, B. Yu, P. Liu and A. M. Abd El-Aty, Antibacterial activity, optical, and functional properties of corn starch-based films impregnated with bamboo leaf volatile oil, *Food Chem.*, 2021, **357**, 129743, DOI: [10.1016/j.foodchem.2021.129743](https://doi.org/10.1016/j.foodchem.2021.129743).
 - 36 R. Farajpour, Z. E. Djomeh, S. Moeini, H. Tavakolipour and S. Safayan, Structural and physico-mechanical properties of potato starch-olive oil edible films reinforced with zein nanoparticles, *Int. J. Biol. Macromol.*, 2020, **149**, 941–950, DOI: [10.1016/j.ijbiomac.2020.01.280](https://doi.org/10.1016/j.ijbiomac.2020.01.280).
 - 37 K. Mustafa, N. Iqbal, S. Ahmad, S. Iqbal, M. Rezakazemi, F. Verpoort and S. Musaddiq, Highly efficient aramid fiber supported polypropylene membranes modified with reduced graphene oxide based metallic nanocomposites: antimicrobial and antiviral capabilities, *RSC Adv.*, 2024, **14**(23), 16421–16431.
 - 38 N. Cebi, M. Arici and O. Sagdic, The famous Turkish rose essential oil: Characterization and authenticity monitoring by FTIR, Raman and GC–MS techniques combined with chemometrics, *Food Chem.*, 2021, **354**, 129495, DOI: [10.1016/j.foodchem.2021.129495](https://doi.org/10.1016/j.foodchem.2021.129495).
 - 39 V. G. L. Souza, I. P. Mello, O. Khalid, J. R. A. Pires, C. Rodrigues, M. M. Alves, C. Santos, A. L. Fernando and I. Coelho, Strategies to improve the barrier and mechanical properties of pectin films for food packaging: Comparing nanocomposites with bilayers, *Coatings*, 2022, **12**, 108, DOI: [10.3390/coatings12010108](https://doi.org/10.3390/coatings12010108).
 - 40 J. Wu, X. Sun, X. Guo, S. Ge and Q. Zhang, Physicochemical properties, antimicrobial activity, and oil release of fish gelatin films incorporated with cinnamon essential oil, *Aquacult. Fish.*, 2017, **2**(4), 185–192, DOI: [10.1016/j.aaf.2017.06.004](https://doi.org/10.1016/j.aaf.2017.06.004).
 - 41 F. Wang, C. Xie, H. Tang, W. Hao, J. Wu, Y. Sun and L. Jiang, Development, characterization and application of intelligent/active packaging of chitosan/chitin nanofibers films containing eggplant anthocyanins, *Food Hydrocolloids*, 2023, **139**, 108496, DOI: [10.1016/j.foodhyd.2023.108496](https://doi.org/10.1016/j.foodhyd.2023.108496).
 - 42 A. M. Youssef and S. M. El-Sayed, Bionanocomposites materials for food packaging applications: Concepts and future outlook, *Carbohydr. Polym.*, 2018, **193**, 19–27, DOI: [10.1016/j.carbpol.2018.03.088](https://doi.org/10.1016/j.carbpol.2018.03.088).
 - 43 J. P. S. Morais, M. de Freitas Rosa, L. D. Nascimento, D. M. Do Nascimento and A. R. Cassales, Extraction and characterization of nanocellulose structures from raw cotton linter, *Carbohydr. Polym.*, 2013, **91**(1), 229–235, DOI: [10.1016/j.carbpol.2012.08.010](https://doi.org/10.1016/j.carbpol.2012.08.010).
 - 44 B. B. Sedayu, P. Wullandari, A. R. Hakim and D. Fransiska, Initial properties identification of refined- and semi refined-carrageenan's as raw materials for biodegradable plastic production, *Squalen Bull. Mar. Fish. Postharv. Biotechnol.*, 2021, **16**(2), 57–64, DOI: [10.15578/squalen.533](https://doi.org/10.15578/squalen.533).
 - 45 Y. Zhang, T. Li, H. Zhang, H. Zhang, Y. Chi, X. Zhao and Y. Wen, Blending with shellac to improve water resistance of soybean protein isolate film, *J. Food Process Eng.*, 2020, **43**(11), e13515, DOI: [10.1111/jfpe.13515](https://doi.org/10.1111/jfpe.13515).
 - 46 S. K. Bhatia, R. Gurav, T. R. Choi, H. R. Jung, S. Y. Yang, Y. M. Moon and Y. H. Yang, Bioconversion of plant biomass hydrolysate into bioplastic (polyhydroxyalkanoates) using *Ralstonia eutropha* 5119, *Bioresour. Technol.*, 2019, **271**, 306–315, DOI: [10.1016/j.biortech.2018.09.12](https://doi.org/10.1016/j.biortech.2018.09.12).
 - 47 Z. J. Zhang, N. Li, H. Z. Li, X. J. Li, J. M. Cao, G. P. Zhang and D. L. He, Preparation and characterization of biocomposite chitosan film containing *Perilla frutescens* (L.) Britt. essential oil, *Ind. Crops Prod.*, 2018, **112**, 660–667, DOI: [10.1016/j.indcrop.2017.12.073](https://doi.org/10.1016/j.indcrop.2017.12.073).
 - 48 T. Huq, S. Salmieri, A. Khan, R. A. Khan, C. Le Tien, B. Riedl and M. Lacroix, Nanocrystalline cellulose (NCC) reinforced alginate based biodegradable nanocomposite film, *Carbohydr. Polym.*, 2012, **90**(4), 1757–1763, DOI: [10.1016/j.carbpol.2012.07.065](https://doi.org/10.1016/j.carbpol.2012.07.065).
 - 49 S. Bhowmik, D. Agyei and A. Ali, Bioactive chitosan and essential oils in sustainable active food packaging: Recent trends, mechanisms, and applications, *Food Packag. Shelf Life*, 2022, **34**, 100962, DOI: [10.1016/j.fpsl.2022.100962](https://doi.org/10.1016/j.fpsl.2022.100962).
 - 50 A. Cendrowski, I. Ścibisz, M. Kieliszek, J. Kolniak-Ostek and M. Mitek, UPLC-PDA-Q/TOF-MS profile of polyphenolic compounds of liqueurs from rose petals (*Rosa rugosa*), *Molecules*, 2017, **22**(11), 1832, DOI: [10.3390/molecules22111832](https://doi.org/10.3390/molecules22111832).
 - 51 M. P. Indumathi and G. R. Rajarajeswari, Mahua oil-based polyurethane/chitosan/nano ZnO composite films for biodegradable food packaging applications, *Int. J. Biol. Macromol.*, 2019, **124**, 268–277, DOI: [10.1016/j.ijbiomac.2018.11.147](https://doi.org/10.1016/j.ijbiomac.2018.11.147).
 - 52 J. F. Mendes, L. B. Norcino, H. H. A. Martins, A. Manrich, C. G. Otoni, E. E. N. Carvalho and L. H. C. Mattoso, Correlating emulsion characteristics with the properties of active starch films loaded with lemongrass essential oil, *Food Hydrocolloids*, 2020, **100**, 105428, DOI: [10.1016/j.foodhyd.2019.105428](https://doi.org/10.1016/j.foodhyd.2019.105428).
 - 53 P. Prajapati, M. Garg, S. Akhtar, T. H. Ansari, R. Chopra, P. Anand and S. D. Sadhu, Development and optimization of active edible coatings to improve the shelf life of Indian soft cheese, *Research Square*, 2023, DOI: [10.21203/rs.3.rs-3176359/v1](https://doi.org/10.21203/rs.3.rs-3176359/v1).
 - 54 M. Bilal, T. Rasheed, F. Nabeel and H. M. Iqbal, Bionanocomposites from biofibers and biopolymers, in: *Biofibers and Biopolymers for Biocomposites: Synthesis, Characterization and Properties*, Springer International Publishing, Cham, 2020, pp. 135–157, DOI: [10.1007/978-3-030-40378-3_7](https://doi.org/10.1007/978-3-030-40378-3_7).
 - 55 M. Abdollahi, S. A. H. Goli and N. Soltanizadeh, Physicochemical properties of foam-templated oleogel based on gelatin and xanthan gum, *Eur. J. Lipid Sci. Technol.*, 2020, **122**(2), 1900196, DOI: [10.1002/ejlt.20190019](https://doi.org/10.1002/ejlt.20190019).
 - 56 S. Karunamay, S. R. Badhe and V. Shulka, Comparative study of essential oil of clove and oregano treated edible film in



- extending shelf life of paneer, *Pharma Innovation*, 2020, **9**, 312–316, DOI: [10.22271/tpi.2020.v9.i7e.4935](https://doi.org/10.22271/tpi.2020.v9.i7e.4935).
- 57 C. Ballester-Costa, E. Sendra, J. Fernández-López and M. Viuda-Martos, Evaluation of the antibacterial and antioxidant activities of chitosan edible films incorporated with organic essential oils obtained from four *Thymus* species, *J. Food Sci. Technol.*, 2016, **53**(8), 3374–3379, DOI: [10.1007/s13197-016-2327-y](https://doi.org/10.1007/s13197-016-2327-y).
- 58 S. A. Dongaree, Y. P. Dige and H. M. Syed, Storage study and textural profile analysis of paneer at different storage temperatures, *Food Sci. Technol. Int.*, 2016, **22**, 153–160.
- 59 I. P. Butler, R. A. Banta, A. A. Tyuftin, J. Holmes, S. Pathania and J. Kerry, Pectin as a biopolymer source for packaging films using a circular economy approach: Origins, extraction, structure and films properties, *Food Packag. Shelf Life*, 2023, **40**, 101224, DOI: [10.1016/j.fpsl.2023.101224](https://doi.org/10.1016/j.fpsl.2023.101224).

